Dy^{3+}-doped $LiYF_4$ crystals for UV-excited white light-emitting diodes

Lei Tang (唐 磊)[1], Haiping Xia (夏海平)[1*], Peiyuan Wang (汪沛渊) [1], Jiangtao Peng (彭江涛)[1], and Haochuan Jiang (江浩川)[2]

[1]*Key Laboratory of Photo-Electronic Materials, Ningbo University,*
Ningbo 315211, China
[2]*Ningbo Institute of Materials Technology and Engineering, Chinese Academy of Sciences,*
Ningbo 315211, China
[*]*Corresponding author: hpxcm@nbu.edu.cn*

Received January 28, 2013; accepted March 29, 2013; posted online May 30, 2013

A Dy^{3+}-doped $LiYF_4$ single crystal capable of generating white light by simultaneous blue and yellow light emission of phosphorescent centers is produced. Chromaticity coordinates and photoluminescence intensity vary with excitation wavelength. Under 350, 365, and 388 nm excitation, the crystal shows excellent white light emission. The most efficient wavelength for white light is 388 nm. The CIE coordinates are x=0.316 and y =0.321, and the color temperature (T_c) is 6 368 K. These results indicate that the studied crystal is a potential candidate for ultraviolet light-excited white light-emitting diodes.

OCIS codes: 160.0160, 230.0230, 300.0300.
doi: 10.3788/COL201311.061603.

White light-emitting diodes (LEDs) have elicited considerable attention as replacements for conventional incandescent and fluorescent lamps in solid-state lighting areas because of their remarkable properties, such as high brightness, rugged structure, lower power consumption, long lifetime span, and environmental benefits[1−3]. Generally, white LEDs are classified into two groups. One group is based on the combination of a YAG:Ce^{3+} yellow phosphor with blue LED chip emitting at 460 nm, and the other is obtained by ultraviolet (UV) light excitation (350 to 420 nm) of a blend of tricolor phosphors[4−6]. The phosphors for white LED applications are usually embedded in epoxy resins. However, this type of white LED has numerous drawbacks. For instance, the refractive indices of the phosphors considerably vary. The heat resistance of the epoxy resin is usually poor. In addition, refractive index mismatch between the phosphors and the epoxy results in light scattering[7].

To overcome these disadvantages, single-phase white light phosphors resulting from the simultaneous emission of blue, green, and red lights under UV light excitation have been developed in borate-based glasses containing Ce^{3+}, Tb^{3+}, and Mn^{2+} as activators[8]. Achieving white light emission using single-host full-color emitting glasses, glass ceramics, and transparent ceramics has drawn considerable attention[9−13]. Many single crystals exhibit good anti-light irradiation, as well as good thermal, mechanical, and chemical stability. The rigid cyclic symmetric structure of single crystals results in the high luminous efficiency of active ions. The excellent thermal, mechanical, chemical, and optical properties of single crystals are beneficial for LED applications to obtain high stability, long lifetime, high luminous efficiency, and good white color. However, only a few reports have focused on rare earth-doped single crystals for LED. $LiYF_4$ crystal doped with rare earth is widely applied as a laser material. Superior properties, such as thermomechanical properties, high optical damage threshold, and wide range transparency[14], render $LiYF_4$ crystal the potential to function as a phosphor for solid-state lighting, specifically, as a phosphor material for white LED.

Rare-earth ions have an important function in display and lighting devices because of their abundant energy levels covering a wide spectral range from the UV to the visible (Vis) region. Numerous rare earth ions, such as Eu^{2+}/Dy^{3+}[15], $Eu^{3+}/Tb^{3+}/Tm^{3+}$[16], and $Tm^{3+}/Ho^{3+}/Yb^{3+}$[17] are used as activators in solid-state materials for white LEDs. Dy^{3+} is well known for its transition in the blue light region at around 480 nm ($^4F_{9/2}\rightarrow{}^6H_{15/2}$) and in the yellow light region at around 573 nm ($^4F_{9/2}\rightarrow{}^6H_{13/2}$) when excited by UV light. These emissions can potentially enable the production of better white LED when a suitable host material is doped with Dy^{3+}ions.

In this letter, we report the growth of Dy^{3+}-doped $LiYF_4$ single crystal by Bridgman method and demonstrate the capability of generating white light by simultaneous yellow and blue emissions of phosphorescent centers under excitation at 388 nm.

The molar composition of the feed material for the doped crystal sample is $0.8DyF_3$-51.5LiF-$47.7YF_3$. The raw material mixture was ground for 1 h in a mortar, sintered with anhydrous HF at 800 °C for 8 h, and then converted into polycrystalline bars. Afterward, moisture and some oxygen impurities in the fluoride powders were removed. The crystals grown by the Bridgman method are approximately 100 mm in length and 10 mm in diameter, as shown in Fig. 1. The crystals are transparent and their purple color deepened with the increase in Dy^{3+} concentration. The detailed growth process and

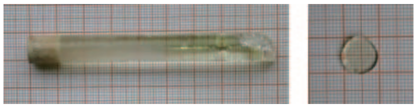

Fig. 1. As-grown Dy^{3+}-doped LiYF$_4$ crystal and polished sample.

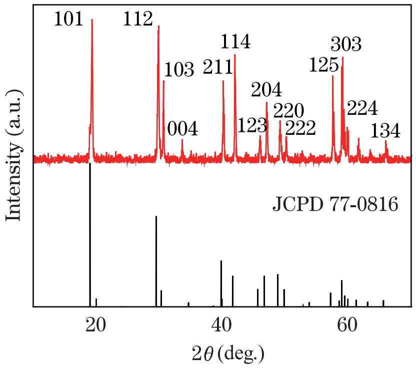

Fig. 2. Powder XRD pattern of Dy^{3+}-doped LiYF$_4$ crystal and standard card of LiYF$_4$ (JCPD No.77-0816).

schematics of the apparatus are very similar to those of the Ce^{3+}:LiYF$_4$ crystal described in Ref. [18]. Along the growth direction, a small pale opaque matter of approximately several centimeters in length at the top of the crystal is observed, corresponding to the final portion of the melt-to-freeze transition. The small pale opaque matter is the eliguation layer, which results from excessive LiF in the starting materials. The as-grown crystals were cut into small pieces and polished well to approximately 3.0-mm thickness for optical measurements. Given the distribution phenomena of Dy^{3+} in the LiYF$_4$ crystal, the concentration of active ions is inhomogeneous. An inductively coupled plasma emission spectrometer was used to measure the concentration of the active ions. The upper part of the Dy^{3+} single-doped LiYF$_4$ crystal has a doping concentration of 0.799 mol% Dy, and the lower part has a doping concentration of 0.795 mol% Dy. The structure was investigated by X-ray diffraction (XRD) using an XD-98X diffractometer (XD-3, Beijing). The absorption spectra were recorded with a spectrophotometer (Lambda 900UV/VIS/NIR Perkin-Elmer, USA) Excitation and fluorescence spectra were measured using a spectrophotometer (F-4500, Shanghai metash instruments, China) from the UV region to the Vis region. All measurements were conducted at 298 K.

The XRD pattern of the Dy^{3+}-doped LiYF$_4$ sample is shown in Fig. 2. Based on the JCPD Card 77-0816, the XRD spectrum shows that the diffraction peaks and relative intensity of the crystal sample are very similar to those of LiYF$_4$. This result indicates that doping with Dy^{3+}has a negligible effect on diffraction data. Thus, the crystal has a pure orthorhombic phase, and the current doping level does not cause any obvious peak shift or second phase. The rare earth ion dopant Dy^{3+} substitutionally enters the Y^{3+} sites.

Figure 3 shows the absorption spectra of the Dy^{3+}-doped LiYF$_4$ single crystals in the wavelength region from 300 to 600 nm and the absorption bands of Dy^{3+} corresponding to the transitions starting from the ground state to the higher levels. The three obvious absorptions around 350, 360, and 388 nm of the Dy^{3+}-doped crystal indicate that the crystal can be efficiently excited by UV light.

Generally, the Dy^{3+} ion possesses energy levels for 480 and 573-nm emissions. To investigate the effect of the exciting band on these emission intensities, excitation spectra were measured. Figure 4 shows the excitation spectra of the Dy^{3+}-doped LiYF$_4$ crystal monitored at 480- and 573-nm wavelengths. The obtained spectra were designated as a and b curves. The excitation spectra of curves a and b in Fig. 4 exhibit similar characteristic bands of Dy^{3+} at 324 ($^6H_{15/2}\rightarrow{}^4M_{17/2}$), 350 ($^6H_{15/2}\rightarrow{}^6P_{7/2}$), 365 ($^6H_{15/2}\rightarrow{}^6P_{5/2}$), and 387 nm ($^6H_{15/2}\rightarrow{}^4I_{13/2}$) when monitored at 480- and 573-nm emissions. The intensity of the excitation bands for curve a is slightly weaker than that for curve b, indicating that the emission intensity at 480-nm wavelength is slightly weaker than that at 573-nm wavelength under excitation at 350, 365, and 388 nm.

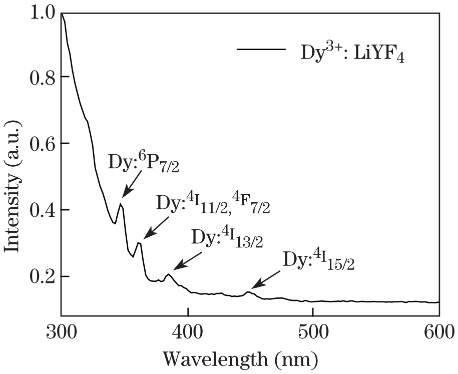

Fig. 3. Absorption spectra of 0.799 mol% Dy^{3+}-doped LiYF$_4$ crystal.

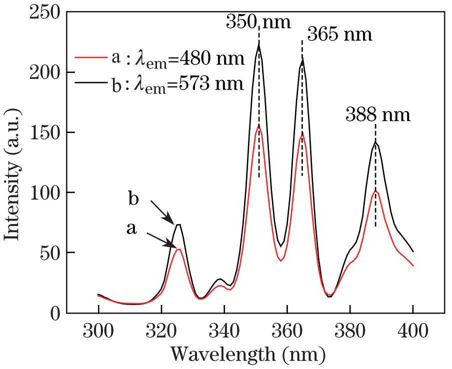

Fig. 4. Excitation spectra of 0.799 mol% Dy^{3+}-doped LiYF$_4$ crystal.

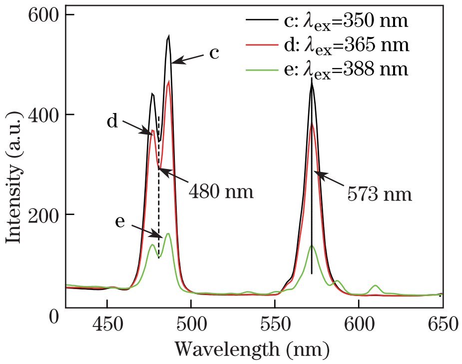

Fig. 5. Emission spectra of 0.799 mol% Dy^{3+}-doped LiYF$_4$ crystal.

The excitation intensities are closely related to the characteristics of the Dy^{3+} ion energy levels and the measured emission wavelength. The result of the excitation spectra corresponds to that of the emission spectra shown in Fig. 5.

The emission spectra of the Dy^{3+}-doped $LiYF_4$ crystal under excitation at 350, 365, and 388 nm were measured and designated as c, d, and e, respectively. Figure 5 shows that under excitation at 350 and 365 nm, the emission spectra of the crystal show a blue band centered at 480 nm ($^4F_{9/2} \rightarrow {}^6H_{15/2}$) and a yellow band at 573 nm ($^4F_{9/2} \rightarrow {}^6H_{13/2}$) of Dy^{3+}. A small yellowish red region at 612 nm ($^5D_0 \rightarrow {}^7F_2$) is observed upon excitation at 388 nm. The emission intensities showing the blue light at 480 nm and the yellow light at 573 nm under 365 and 388-nm excitations are weaker than that under 350-nm excitation. However, the red light emission intensity at 612 nm is generated only under excitation at 388 nm. These results confirm that blue, yellow, and red lights can be simultaneously obtained from Dy^{3+}-doped $LiYF_4$ crystals excited with appropriate UV light. The CIE chromaticity coordinates of the Dy^{3+}-doped $LiYF_4$ crystal calculated from the corresponding emission spectrum are summarized in Table 1. Excitation at 388 nm shows better results than that at 350 and 365 nm.

Figure 6 presents the emission spectra of the upper (0.799 mol%) and lower parts (0.795 mol%) of the Dy^{3+}-doped $LiYF_4$crystal. The parts show similar pattern with slightly different relative intensities. The upper part emission spectra intensity is stronger than the lower part. In addition, the shape and position of emission peaks are not influenced by the excitation wavelength.

The CIE chromaticity coordinates for the different parts of the Dy^{3+}-doped $LiYF_4$ crystal under 388-nm excitation are illustrated in Fig. 7. The coordinates are calculated using the corresponding emission spectrum in Fig. 6. Upon excitation at 388 nm, the lower part of the crystal emits white light (point f; CIE coordinate $x = 0.303$, $y = 0.320$) and the upper part emits pure white light (point e; CIE coordinate $x = 0.316$, $y = 0.321$). The color temperature T_c=7 165 K can be obtained from the color temperature calculation software for $x = 0.303$, $y = 0.320$, and $T_c = 6\,368$ K for $x = 0.316$, $y = 0.321$. Therefore, emission color can be tuned by varying the excitation wavelengths and relative concentration of Dy^{3+} based on the excitation and emission spectra, as well as CIE chromaticity coordinates. White light emission can be obtained from the Dy^{3+}-doped $LiYF_4$ crystal excited with appropriate UV light.

Table 1 Comparison of CIE Chromaticity Coordinates of 0.799 mol% Dy^{3+}-doped $LiYF_4$ Single Crystall

Serial Number	λ_{ex} (nm)	(x, y)
c	350	(0.281, 0.334)
d	365	(0.278, 0.327)
e	388	(0.316, 0.321)

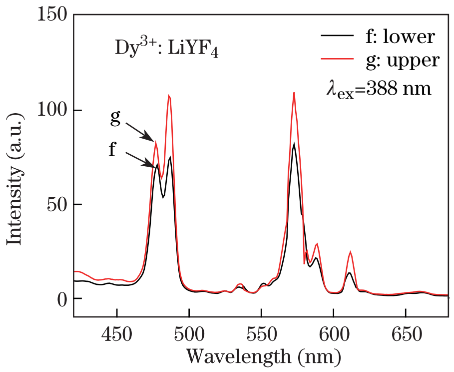

Fig. 6. Emission (λ_{ex}=388 nm) spectra of Dy^{3+}-doped $LiYF_4$ crystal.

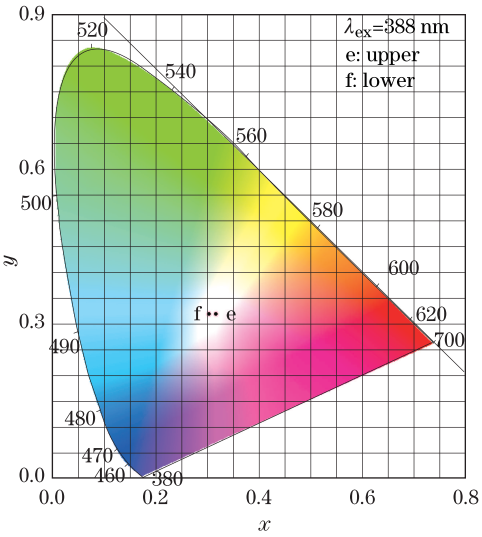

Fig. 7. CIE chromatic coordinate diagram of Dy^{3+}-doped $LiYF_4$ crystal.

In conclusion, Dy^{3+}-doped $LiYF_4$ single crystals with good quality and optical properties can be synthesized by Bridgman method. The Dy^{3+}-doped $LiYF_4$crystals exhibit intense emission bands in the near blue region from 470 to 490 nm and in the yellow region from 570 to 600 nm. A small red region is observed from 600 to 615 nm under excitation at 388 nm. Under excitation at 350, 365, or 388-nm wavelength light, white light emission is achieved. White light is obtained with the highest efficiency at 388 nm. Moreover, the color of luminescence can be adjusted by varying the excitation wavelength and the doping concentration of Dy^{3+}. Therefore $LiYF_4$ crystal doped with Dy^{3+} is a promising phosphor for white LED.

This work was supported by the National Natural Science Foundation of China (Nos. 51272109 and 50972061), the Natural Science Foundation of Zhejiang Province (Nos. R4100364 and Z4110072), the Natural Science Foundation of Ningbo City (No. 2012A610115), and the K. C. Wong Magna Fund in Ningbo University.

References

1. E. F. Schubert and J. K. Kim, Science **308,** 1274 (2005).
2. K. Sakuma, S. Hirafune, K. Asano, N. Hiroski, and R. J. Xie, Appl. Phys. Lett. **90,** 051109 (2007).
3. M. Zeuner, F. Hintze, and W. Schnick, Chem. Mater. **21,** 336 (2009).
4. M. Zhang, J. Wang, W. Ding, Q. Zhang, and Q. Su,

Appl. Phys. B **86,** 647 (2007).

5. K. Deng, T. Gong, Y. Chen, C. Duan, and M. Yin, Opt. Lett. **36,** 4470 (2011).
6. P. Xu, C. Xia, F. Wu, X. Li, Q. Sai, G. Zhou, and X. Xu, Chin. Opt. Lett. **10,** 021601 (2012).
7. Z. Cui, G. Jia, D. Deng, Y. Hua, S. Zhao, L. Huang, H. Ma, and S. Xu, J. Lumin. **132,** 153 (2012).
8. J. C. Zhang, C. Parent, G. Le Flem, and P. Hagenmuller, J. Solid State Chem. **93,** 17 (1991).
9. C. Zhao, J. Cai, R. Li, S. Tie, X. Wan, and J. Shen, J. Non-Cryst. Solids **358,** 604 (2012).
10. C. Zhu, Y. Yang, X. Liang, S. Yuan, and G. Chen, J. Lumin. **126,** 707 (2007).
11. R. Wei, H. Zhang, F. Li, and H. Guo, J. Am. Ceram. Soc. **95,** 34 (2012).
12. T. Nakanishi and S. Tanabe, Phys. Status Solidi A **206,** 919 (2009).
13. X. Hou, S. Zhou, T. Jia, H. Lin, and H. Teng, J. Alloys Compd. **509,** 2793 (2011).
14. L. Gomes, A. F. H. Librantz, F. H. Jagosich, W. A. L. Alves, I. M. Ranieri, and S. L. Baldochi, J. Appl. Phys. **106,** 103508 (2009).
15. R. Ye, Z. Cui, Y. Hua, D. Deng, S. Zhao, C. Li, and S. Xu, J. Non-Cryst. Solids **357,** 2282 (2011).
16. C. Zhao, J. Cai, R. Li, S. Tie, X. Wan, and J. Shen, J Non-Cryst Solids **358,** 604 (2012).
17. H. Gong, D. L. Yang, X. Zhao, E. Y. B. Pun, and H. Lin, Opt. Mater. **32,** 554 (2010).
18. Y. Katayama and S. Tamabe, Opt. Mater. **33,** 176 (2010).